

A NEW METHOD OF ABSORPTION-PHASE NANOTOMOGRAPHY FOR 3D OBSERVATION OF MINERAL-ORGANICS-WATER TEXTURES AND ITS APPLICATION TO PRISTINE CARBONACEOUS CHONDRITES. A. Tsuchiyama¹, A. Nakato¹, J. Matsuno¹, M. Sugimoto¹, K. Uesugi², A. Takeuchi², T. Nakano³, E. Vaccaro⁴, S. Russel⁴, K. Nakamura-Messenger⁵, A. S. Burton⁵, S. Messenger⁵, A. Miyake¹, A. Takigawa^{1,6}, A. Takayama¹, ¹Division of Earth and Planetary Sciences, Graduate School of Science, Kyoto University, Kyoto, JAPAN (atsuchi@kueps.kyoto-u.ac.jp), ²JASRI/SPring-8, Sayo, JAPAN, ³GSJ/AIST, Tsukuba, JAPAN, ⁴National History Museum, London, UK, ⁵Astrominerals Research and Exploration Science Division, NASA JSC, Houston, TX, USA, ⁶The Hakubi Center for Advanced Research, Kyoto University, Kyoto, JAPAN,

Introduction: Pristine carbonaceous chondrites contain fine-grained matrix, which is composed largely of amorphous silicates, sub-micron silicate and sulfide crystals, and organic materials (e.g., [1]). They are regarded as primitive dust in the early Solar System that have suffered minimal alteration in their parent bodies. The matrix generally has different lithologies; some of them are unaltered but some are more or less aqueously altered (e.g., [2]). Their textures have been examined in 2D usually by FE-SEM/EDS, TEM/EDS, nano-SIMS and micro-XRD [3]. Observation of their complex fine textures, such as spatial relation between different lithologies in 3D, is important for understanding aggregation and alteration processes.

Synchrotron radiation (SR)-based X-ray tomography reveals 3D structures nondestructively with high spatial resolution of ~ 100 nm. We have developed a new technique using absorption contrasts called “dual-energy tomography” (DET) to obtain 3D distribution of minerals at SPring-8, SR facility in Japan [4], and applied successfully to Itokawa particles [5]. Phase and absorption contrast images can be simultaneously obtained in 3D by using “scanning-imaging x-ray microscopy” (SIXM) at SPring-8, which can discriminate between void, water and organic materials [6]. We applied this technique combined with FIB micro-sampling to carbonaceous chondrites to search for primitive liquid water [7]. In this study, we combined the DET and SIXM to obtain three dimensional submicron-scale association between minerals, organic materials and water and applied this to pristine carbonaceous chondrites.

DET, SIXM and their combined method: Refractive index is expressed by $n=1-\delta+i\beta$, where the real part, $1-\delta$, is the refractive index with decrement (RID), δ , which is nearly proportional to the density, ρ , and the imaginary part, β , is the extinction coefficient, which is related to the linear attenuation coefficient (LAC), $\mu = \rho \sum \tau_i w_i$, where $\tau_i(E)$ is the mass attenuation coefficient of element i , as a function of the X-ray energy and w_i is the weight fraction of element i . Spatial distributions of RIDs and LACs are obtained as digital images (CT images) by phase and absorption tomography, respectively.

In DET, mineral phases can be discriminated based on the LACs obtained at the two different energies (e.g., 7 and 8 keV) [4]. As the K-absorption edge of Fe is 7.11 keV, LACs at 8 keV increase more largely than 7 keV with increasing the Fe content of a phase, while the LACs of Fe-free phases at 7 and 8 keV changes similarly. In SIXM, the phase and absorption contrast images (RID and LAC images) can be obtained simultaneously at a single x-ray energy (8 keV) [6,7]. As materials composed of light elements such as organic materials or water have very low LACs, they cannot be identified from void. In contrast, they can be discriminated based on the RIDs due to the density differences.

By combining DET and SIXM, more detailed information including minerals, organic materials (or water) and voids can be obtained in 3D. In this method, it is important to consider (1) calibration of LAC and RID values and (2) registration of LAC and RID images. (1) It has been known that the LAC values in CT images, μ_{CT} , is proportional to the theoretical LAC values, μ ; $\mu_{CT} = \gamma\mu$, where γ is an empirical constant (0.887 ± 0.004 at SPring-8) [4]. RID and LAC values in SIXM were also calibrated using standard materials; $\gamma = 0.909 \pm 0.006$ for RID and 0.909 ± 0.008 for LAC at SPring-8. (2) Because the size of the voxel (pixel in 3D) of CT images at different energies in DET and SIXM are different, the locations of an object in the two images are matched with the same voxel size (image registration). Manual image registration is a time-consuming procedure [4] and thus in this study, we have developed a new method to perform image registration semi-automatically. Then, we can investigate qualitatively LAC and RID values in matched CT image sets by DET and SIXM.

Application to pristine carbonaceous chondrites:

The samples used in the present study are Acfer 094 (C2 ungrouped), Miller Range (MIL) 07687 (CO3), Miller Range (MIL) 090657 (CR2.7) and Queen Alexandra Range (QUE) 99177 (CR2). Prior to CT imaging experiments, cross sections of polished thin sections or potted butts of the samples were carefully examined by FE SEM with high spatial resolution with EDS for elemental mapping (JEOL JSM-7001F/X-Max150) to choose regions of interest (ROIs). Then, a block 20-30

μm in size was picked up from a ROI by FIB (FEI Helios nanolab G3 CX/OCtane Elite 25 and FEI Quanta 200 3DS) [8]. The blocks were imaged by DET and SIXM at BL47XU of SPring-8 with the voxel sizes of ~ 35 and ~ 40 nm (~ 70 and ~ 80 nm for larger samples) at 7 and 8 keV in DET, respectively, and ~ 100 nm at 8 keV in SIXM. The image registration was performed among DET and SIXM images.

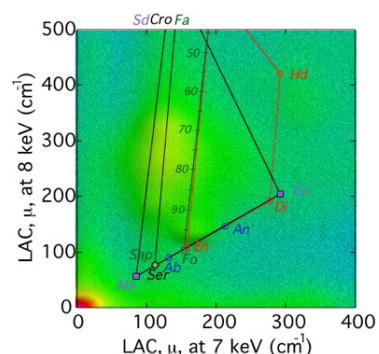


Figure 1. An example of 2D histogram of LAC at 7 and 8 keV of MIL 090657. Ms: magnesite, Sd: siderite, Sap: saponite, Ser: serpentine, Cro: cronstedtite.

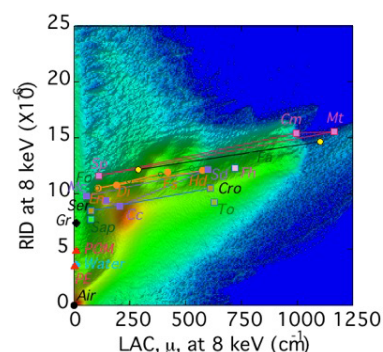


Figure 2. An example of 2D histogram of LAC and RID at 8 keV (SIXM) of Acfer 094. To: tochilinite, Fh: ferrihydrite, POM: polyacetal, PE: polyethylene.

corresponds to a less altered lithology with high porosity. We recognized another lithologies based on the difference in color. The lithology on the lower half of the sample (B in Fig. 4b) has higher porosity and richer in Fe than the lithology on the surface (A in Fig. 4b). Their boundary is wavy in 3D and not very sharp, but the lithology changes within $\sim 1 \mu\text{m}$. We also recognized a highly porous lithology (or small inclusion) with sharp boundary in the bottom portion of the sample (C in Fig. 4c). The lithologies B

The matched DET and SIXM image sets were examined. 2D histograms for LACs at 7 and 8 keV (Fig. 1) and RID-LAC at 8 keV (Fig. 2) were obtained to estimate mineral phases. Organic materials were also observed in phase contrast images (Fig. 3).

Color images were made from the matched image sets. Figure 4 show an example of color maps of Acfer 094, where 7, 8 keV (DET) and phase (SIXM) images were applied to R, G and B, respectively. SEM/EDS analysis of this sample showed that the surface of the thin section (the left and top sides of Figs. 4b and c, respectively) corresponds to a less

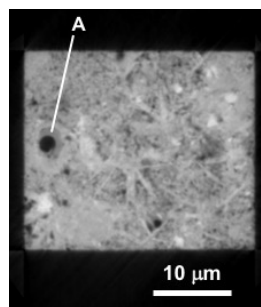


Figure 3. Organic material with pore (A) in a mildly altered lithology of MIL 07687 (phase image).

and C were not observed by the SEM/EDS observation on the surface.

In other samples, many lithologies having different textures with different porosity and Fe contents, which correspond to different alteration, were recognized from DET-SIXM images as shown in Figure 4. Some of them were not observed on the surface. The present results show that the pristine carbonaceous chondrites have more complicated micro textures in the matrix with a variety of lithologies than expected from the 2D observations using SEM/EDS. In future work, we plan to examine these samples with TEM (conventional and tomography) by FIB sampling based on the 3D structures obtained in this study. We can detect water not only as hydrous phases but also liquid water using this technique. This technique has potential availability for Hayabusa-2 sample analysis too.

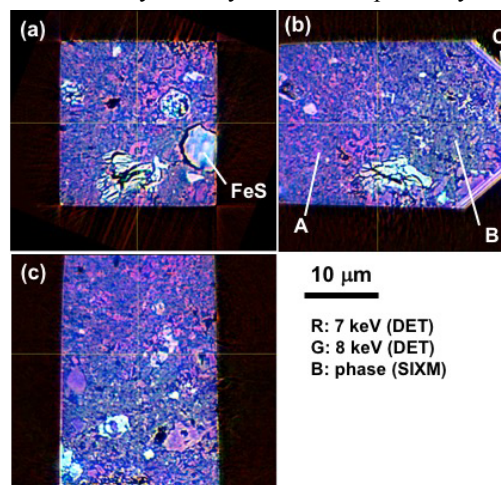


Figure 4. An orthogonal view of color maps (Acfer 094). Three different lithologies (A, B and C) can be recognized.

References: [1] Scott E. and Krot A. (2007) *Treatise on Geochemistry* 1-72. [2] Leroux H. et al. (2015) *GCA*, 170: 247-265. [3] Vaccaro E. et al. (2015) *MetSoc. Abstract #5264*. [4] Tsuchiyama A. et al. (2013) *GCA*, 116: 5-16. [5] Tsuchiyama, A. et al., (2011) *Science*, 333, 1125-1128. [6] Takeuchi A. et al. (2013) *J. Synch. Rad.*, 20: 793-800. [7] Tsuchiyama, A. et al. (2016) *Goldschmidt Conf.*, Abstract #3193. [8] Miyake et al. 2014, *Microscopy*, 63: i24.